

# Instantly investigating the adsorption of polymeric corrosion inhibitors on magnesium alloys by surface analysis under ambient conditions

L. M. G. Gonçalves<sup>1,a,b</sup>, L.C. Sanchez<sup>1,a,b</sup>, S. Stamboroski<sup>1,a,c</sup>, Y. R. Corrales Urena<sup>1,d</sup>, W. Leite Cavalcanti<sup>1,\*</sup>, J. Ihde<sup>1</sup>, M. Noeske<sup>1</sup>, M. Soltau<sup>2</sup>, K. Brune<sup>1</sup>

<sup>1</sup> Fraunhofer Institute for Manufacturing Technology and Advanced Materials - IFAM, Bremen, Germany

<sup>a</sup> CAPES Foundation, Ministry of Education of Brazil, Brasília - DF

<sup>b</sup> Department of Materials Engineering, UFSCar, Federal University of São Carlos, São Carlos, Brazil

<sup>c</sup> Department of Chemistry, UFSC, Federal University of Santa Catarina, Florianópolis, Brazil

<sup>d</sup> UNESP São Paulo State University, São Paulo, Brazil

<sup>2</sup> Straetmans High TAC GmbH, Hamburg, Germany

Email: \*welchy.leite.cavalcanti@ifam.fraunhofer.de

Received \*\*\*\* 2014

Copyright © 2014 by author(s) and Scientific Research Publishing Inc.

This work is licensed under the Creative Commons Attribution International License (CC BY).

<http://creativecommons.org/licenses/by/4.0/>



---

## Abstract

Surface engineering of magnesium alloys requires adequate strategies, processes and materials permitting corrosion protection due the high reactivity. Liquid formulations containing corrosion inhibitors often are to be optimized according to the demands of the respective substrate and its application. As an interdisciplinary approach, a combination of several techniques for instantly monitoring or elaborately analyzing the surface state of magnesium was accomplished in order to characterize the performance of new adsorbing sustainable amphiphilic polymers which recently were developed to facilitate a multi-metal corrosion protection approach. The application of established techniques like Contact Angle measurements and X-ray Photoelectron Spectroscopy was supplemented by introducing related and yet faster online-capable and larger-scale techniques like Aerosol Wetting Test and Optically Stimulated Electron Emission. Moreover, an inexpensive set-up was configured for scaling the inset and the extent of degradation processes which occur at local electrochemical circuits and lead to hydrogen bubble formation. Using these analytical tools, changes of the surface state of emiered AM50 samples were investigated. Even in contact with water, being a moderate corrosive medium, the online techniques facilitated detecting surface deg-

---

\*Corresponding author.

radiation of the unprotected magnesium alloy within some seconds. In contrast, following contact with a 1 wt% formulation of a polymeric corrosion inhibitor, surface monitoring indicated a delay of the onset of degradation processes by approximately two orders of magnitude in time. Mainly based on the spectroscopic investigations, the corrosion inhibiting effects of the investigated polymer are attributed to the adsorption of a primary polymer layer with a thickness of a few nanometers which occurs within some seconds. Immersion of magnesium for several hours brings up a protective film with around ten nanometers thickness.

## Keywords

Online surface monitoring; magnesium alloys; polymeric corrosion inhibitors; fast screening of effective formulations; optimization of application process

## 1. Introduction

Magnesium alloys have been used in transport and especially automotive industries due to their providing a combination of light weight and high specific strength. Magnesium is also an excellent functional material. Its alloys are attractive battery electrodes, sacrifice anodes, and hydrogen storage material. However, when exposed to ambient atmosphere and wet environments unprotected magnesium is too reactive and susceptible to corrosion [1]. Evidently, applications and devices profiting from the structural properties of magnesium alloys must be reliable [2]. In this way, corrosion protection is a relevant aspect to be considered.

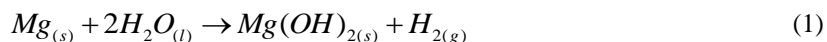
A large amount of approaches based on material engineering have been used to improve the corrosion resistance of Magnesium alloys, for example decreasing impurity level, increasing the amount of Aluminum and producing a more homogeneous microstructure by rapid solidification [3,4]. Furthermore, nanostructured superhydrophobic films [5], self-assembled monolayers [6], and polymeric corrosion inhibitors have been shown to provide corrosion protection for different types of metals. Inhibitors are often easy to apply and offer the advantage of in-situ application without causing any significant disruption to the process [3].

Different analytical techniques have been used to investigate the corrosion behaviour of Magnesium alloys. X-ray Photoelectron Spectroscopy (XPS) is a vacuum-based technique for surface analysis providing insight in the elemental and chemical composition of an approximately ten nanometer thin surface layer, and XPS is established for evaluating the performance of corrosion protection systems for magnesium alloys [5,6]

Aiming at instant online analysis under ambient conditions, secondary electron emission or the interaction between magnesium (alloy) surfaces and water may be assessed.

Optically stimulated electron emission (OSEE) may be considered a non-destructive technique to detect contaminants on adherent surfaces due to the change of electron emission characteristics, e.g. the work function [7]. Modifications of the surface state of metals [8] or metals covered with self-assembled monolayers (SAM) [9], ceramics [10], polymers and also CFRP [11] may result in a change of the detected electron flow [12,13]. In case of metals, the presence of nonconductive substances or films on the surface would interfere with the surface photoemission, resulting in a lower value read in the scale of arbitrary units [14]. This OSEE ability of giving evidence about layers on surfaces may be useful, for instance, to determine the optimal duration of surface treatments for various substrates, as degreasing or etching. However, the technique alone will not be able to clearly discriminate effects of different surface treatments, since identical values may be obtained from different surface chemical states [9]. In this way, the technique is supposed to work in its best condition when it only differentiates an initial and a final surface by the presence or absence of a surface contaminant [14]. On the other hand, the device is also capable of following the effects of a surface treatment as a function of time, as for example to determine the growth law of an oxide film on the surface of freshly emiered copper [9].

Upon interaction between water and magnesium (alloy) surfaces, hydrogen is formed resulting from the corrosion of magnesium. The overall reaction for the corrosion of magnesium can be expressed as Equation (1) [1].



A protic electrolyte in contact with an aluminum [15] or magnesium alloy may locally become supersaturated due to the fast formation of hydrogen upon metal degradation. In this way, around local galvanic cells hydrogen bubbles may be formed [15].

Based on this principle, a procedure shortly called Hydrogen Bubble Formation Test (H<sub>2</sub>BT) was set up and used to observe and follow inset and extent of hydrogen bubble formation on magnesium alloy. Using a digital light microscope videos were recorded and images of several appearing, growing and finally ascending hydrogen bubbles were evaluated.

Moreover, wetting properties of magnesium surfaces can be investigated. Theoretically, on an ideal flat, rigid and homogeneous surface the contact angle ( $\Theta_\gamma$ ) is used to determine surface energy and surface tension to described solid–liquid interactions [16]. The contact angle ( $\Theta_\gamma$ ) of a liquid drop on a solid surface is defined by the mechanical equilibrium of the drop under the action of three interfacial tensions( $\gamma$ ): solid-vapor  $\gamma_{sv}$ , solid-liquid  $\gamma_{sl}$  and liquid-vapor  $\gamma_{lv}$ . This equilibrium relation described in Equation (2) is known as Young's equation [17].

$$\gamma_{lv} \cos \theta_\gamma = \gamma_{sv} - \gamma_{sl} \quad (2)$$

In general the surface energy of a material depends on the chemical composition and surface charge [18]. In not ideal conditions the contact angles values depend do not only on the surface energy between the interfaces [19] but are also influenced by the surface geometry of the solid which changes depending of roughness [19] and type of porosity [20]. A non-spectral method like the contact angle is a simple, rapid and inexpensive technique used extensively to characterize changes in the surface wetting behavior [21] due to processes for surface modification [22] or surface contamination [16]. The water contact angle indicates the surface wettability based on the spreading behavior of the droplet of water on a surface [21].

The Aerosol Wetting Test (AWT) is a method to rapidly characterize the wetting properties of large-scale surfaces with a frequency of around 0.001 m<sup>2</sup>/s [23]. This technique was developed to overcome some limitations of contact angle measurements with respect to their speed and the limitations of the fast water break test with respect to obtaining continuous quantitative data. With AWT, two sides of a sample can be measured separately, curved surfaces can be investigated, large samples can be measured, and a quick access to surface wettability maps is facilitated. Moreover, the AWT adds high material throughput due to measuring areas of approximately ten square centimeters in less than five seconds.

The expedient applicability of the AWT for identifying regions covered with release agent or hydraulic fluid and, as another scenario, thermally degraded surfaces was reported for Carbon-Fiber Reinforced Composite (CFRP) substrates in the frame of an extended Non-Destructive Testing (ENDT) approach [24–26]. However, investigations concerning the potential of the AWT to detect the presence of corrosion inhibiting layers or to investigate early stages of corrosion starting from a material interface were not yet reported.

In this work, for the first time a combination of several techniques for monitoring or analyzing the state of metal surfaces was used to investigate magnesium corrosion protection, reporting the potential of new adsorbing sustainable amphiphilic polymers which recently were developed to facilitate a multi-metal corrosion protection approach. Hydrogen Bubble Formation Test (H<sub>2</sub>BT), Contact Angle (CA), Aerosol Wetting Test (AWT), Optically Stimulated Electron Emission (OSEE) and X-Ray Photoelectron Spectroscopy (XPS) were applied to investigate the surface state of emiered AM50 samples covered with a polymeric corrosion inhibitor.

## 2. Experimental Procedure

Samples of AM50 alloy (Rocholl GmbH, Aglasterhausen, Germany) were cut and manually emiered using dry and flat SiC sandpaper with a grit size of 800 mesh, in order to create a fresh surface under ambient conditions. After grinding, two sets of samples were investigated. The first set comprises samples which were immersed in demineralized water, and the samples of the second set were immersed in an aqueous liquid formulation containing 1 wt% of polymeric corrosion inhibitor (p.c.i). The investigated times of immersion were 5, 10, 30, and 90 seconds, 3, 10 and 30 minutes (180, 600 and 1800 s, respectively), 1, 3 and 6 hours (3600, 10800 and 21600 s, respectively). After the pre-defined times of immersion, samples were withdrawn from the formulation, and the liquid film was blown away from surface using air pressurized with a hand bellow. In case of the second set

of samples, which were immersed in the formulation to be investigated with respect to its corrosion inhibiting effects, freshly immersed sample specimens were submitted to water rinsing for 25 seconds. This procedure was applied in order to remove possibly remaining physisorbates on the surface before the drying with a bellow. Sketches of both procedures are shown in **Figure 1**.

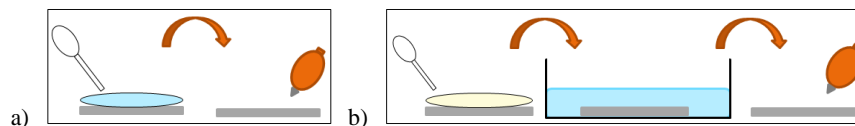


**Figure 1.** a) Sketch of water immersion procedure; b) Sketch of corrosion inhibitor in liquid formulation immersion procedure.

One portion of each set of samples were next scanned with the OSEE technique and imaged with the AWT technique, and then a cut sample piece was taken to XPS measurements. Another portion of samples was characterized with measurements of contact angle (CA) or Hydrogen bubble formation test ( $H_2BT$ ).

For the CA and AWT measurements, Silicon (110) wafer and Glassy Carbon samples were used as reference samples to verify the reproducibility of the water deposition in both tests. Both samples were used as received, with no cleaning process done before measurements to guarantee that the process wouldn't differentiate the surface in different days of measurements.

## 2.1. Description of the polymeric corrosion inhibitor (p.c.i.) solution

A water-based formulation G50 wb of Additive G50 (Straetmans High TAC GmbH, Hamburg, Germany) was used. Based on a 50 wt% containing parent formulation, a 1 wt% formulation was prepared by diluting the parent solution with demineralised water. Attached to a polymeric polyoxyalkylene backbone, the metalophilic anchors comprised in polymers of the G50 type are the conjugate base of acidic groups [27]. The polar groups of the amphiphilic polymers may interact with various cations in oxide, hydroxide or carbonate-based reaction layers on distinct metals and alloys. The development of such multi-metal protection capacity of the amphiphilic polymers which are contained in G50 wb was governed by computer-based simulation [28].

## 2.2. Contact Angle (CA)

The apparent contact angles were measured using a goniometer (OCA15 Plus, Data Physics Instruments, Germany) by sessile drop technique and HPLC grade water (Across Organics) was used as probe liquid; the volume of the drops was kept constant (20 $\mu$ l) for each measurement. The contact angle values reported are an average value of at least nine separate drops on different substrates area. The recorded images were analyzed by SCAN 20 Data Physics software.

## 2.3. Aerosol Wetting Technique (AWT)

When applied to surfaces, droplets of an aerosol can form wide or narrow drops, according to the surface state and surface energy. The Aerosol Wetting Test can be related to the CA principles and measurements: for a defined liquid volume, the droplet size depends directly on the contact angle [26]. In this case the droplet diameter is measured instead of the contact angle itself. In the **Figure 2**, the relation between the contact angle and the drop diameter is illustrated. This means that the property of a surface to be wetted can be characterized by the droplet size distribution.

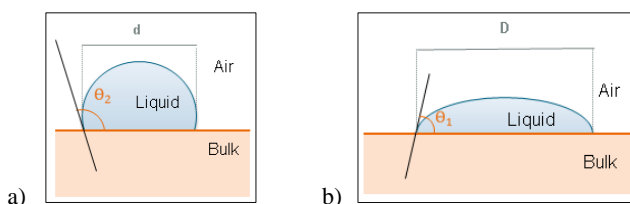


**Figure 2.** Sketch of the relation between the contact angle and drop size diameter where  $D$  and  $d$  are the drop diameter (with  $d < D$ ), and  $\theta_1$  and  $\theta_2$  are the contact angles ( $\theta_1 < \theta_2$ ). **a)** Higher contact angles and poor wetting, with smaller drop sizes; **b)** smaller contact angles, higher wetting and bigger drop sizes.

As a quick résumé, higher contact angles imply poor wetting and smaller drop sizes ([Error! Reference source not found..a](#)); and smaller contact angles imply higher wetting and bigger drop sizes ([Error! Reference source not found..b](#)). If the surface energy of a sample (locally) is low, e.g. due to contaminations like release agents (silicones, fluoropolymers), narrow drops will be formed on the surface. If the surface energy of a sample is high, wide drops will form [26]. The Aerosol Wetting Test evaluates the mean drop size of droplets after application of an aerosol.

The Aerosol Wetting Test system consists on a spray-mist ultrasonic atomizer, a linear motion table, an illumination unit composed by parallel lights, an image detection system and a computer with software for image analysis. Small primary water drops with a narrow drop size distribution, forming a fog, were created using an ultrasonic atomizer nozzle (Sonotek, Impact, 120 kHz). This nozzle was fed by a syringe pump (Sonotek 997) ensuring a constant water flow of 5.0 ml/min. With a constant airflow, these drops were sprayed towards the sample surface, which was exposed to the spray for one cycle with two applications. Depending on the surface energy of the sample, these drops form a particular pattern, with wide or narrow secondary drops (formed by confluence of primary drops) on the surface. A camera (Olympus, ColorView III,  $2576 \times 1932$  pixels<sup>2</sup>, field of view:  $13 \times 10$  mm<sup>2</sup>), positioned perpendicularly to the surface, was used to acquire images of these drop patterns in a pre-selected region of the tested surface. The pictures were processed (background subtraction and quality refining) using an image analysis software (Soft Imaging System, analySIS 5.0). This step is necessary to remove structures or scratches on the sample. Afterwards, the perimeters of the drops were identified, and the areas of the drops were measured and classified. Using a two parameter fit, the results were fitted to match a Rosin-Rammler drop-size distribution [24]. The mean distribution width was used to rate the fitting results. The results obtained for each condition were compared among themselves and statements about the wetting properties were done [23].

## 2.4. Hydrogen Bubble Formation Test (H<sub>2</sub>BT)

Using a microscope Keyence VHX500 under ambient conditions, samples with a size of  $25\text{mm} \times 25\text{mm}$  were submitted to the H<sub>2</sub>BT. A sample was placed on the table of the microscope, and a silicon mold with an opening with a diameter of 10mm was pressed against the sample surface as depicted in [Figure 3](#). Images were taken before and during the contact of the AM50 surface with ca. 0.27 mL of water or the aqueous G50wb formulation. Videos with duration of ten minutes were recorded. Light microscopic images of the initial and the final state of the sample surface were taken. Before each measurement the mold was cleaned with pure water and isopropanol in order to guarantee that no silicone material, which might influence the corrosion behavior of the sample, becomes released from the mold. Additionally, the wetting behavior of samples having passed the H<sub>2</sub>BT was inspected with the AWT.

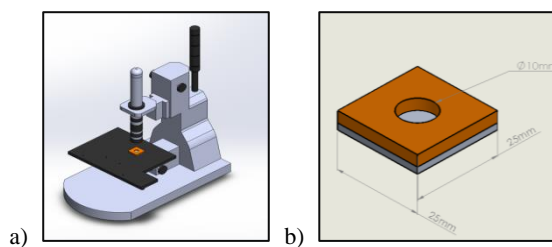


**Figure 3.** Sketches of the Hydrogen Bubble Formation Test (H<sub>2</sub>BT) experimental procedure; a) Set-up with sample on microscope table; b) metal sample with silicone mould on top.

## 2.5. Optically Stimulated Electron Emission (OSEE)

OSEE experiments were performed under ambient conditions with a Surface Quality Monitor SQM200 (Photo Emission Tech., Inc. (PET), USA). During an OSEE measurement, the sample surface is exposed to ultra-violet light of a mercury vapor lamp with wavelength maxima of 254 and 187 nm, corresponding to 4.9 and 6.7 eV. The emitted photoelectrons exhibit kinetic energy of less than approximately 2 eV which effects a sub-micrometer information depth for the surface of a solid and an interaction with the atmosphere as low as to permit sensor-surface distances in the millimeter range. An electric potential of 40V causes the attraction of the emitted photoelectrons to the collector, generating a current which is measured by a solid state electrometer. The measured photocurrent values are converted to a scale of arbitrary units, denoted as OSEE intensity, and may be interpreted in terms of integral band intensities of the underlying contributing electronic spectra [29], appending the respective photoionization cross sections. The device is operated with a moving table, electrically conductive and earthed, in which samples are placed during the procedures. Due to sample dimensions in the range of 25mm × 25 mm, an aperture of 1.6mm diameter was used in front of the UV lamp standing about 5.5 mm from the surface. The samples were scanned with a step size of 1.016 mm in orthogonal directions, covering the whole sample area. For purposes of evaluation, a mean OSEE signal value was calculated by averaging the OSEE intensities obtained within an area of 10 mm × 10 mm on the central portion of the sample. For each time of immersion of magnesium samples, measurements in different samples were repeated at least three times and an average of all measurements realized were plotted along with the thus obtained standard deviation.

## 2.6. X-ray Photoelectron Spectroscopy (XPS)

The XPS spectra were taken using a Kratos Ultra system applying the following acquisition parameters: base pressure:  $4 \cdot 10^{-8}$  Pa, sample neutralization applying low energy electrons (<5 eV), hybrid mode (electrostatic and magnetic lenses are used), take off angle of electrons  $0^\circ$ , pass energy 20 eV (or, respectively, 40 eV in case of some less concentrated constituents) in high resolution spectra and 160 eV in survey spectra, excitation of photoelectrons was done by monochromatic AlK<sub>α</sub> radiation. The analysis area is elliptically shaped with main axes of 0.3 mm × 0.7 mm. The binding energy calibration of the electrically isolating polymer was performed by referring the C1s component of aliphatic carbon species to 285.0 eV. Elemental ratios were calculated based on the area of the peaks and considering the percentage of the elements provided by XPS.

## 3. Results and Discussions

In this chapter, the results obtained when investigating the changes of AM50 surfaces in contact with water or with an aqueous G50wb formulation containing a polymeric corrosion inhibitor (p.c.i.) will be reported. Special focus will be put to experimental and analytical procedures revealing changes within a few minutes. Based on details about the adsorption behavior of p.c.i. molecules, the chronology and the effects resulting from the interaction of p.c.i. with AM50 surfaces will be elaborated.

### 3.1. Simulations of the dynamical behaviour of a polymeric corrosion inhibitor

Investigations based on Dissipative Particle Dynamics (DPD) simulations indicate that the attachment of the

first layer of G50 type p.c.i. polymers to hydrophilic surfaces formed by reaction layers occurs via the polar groups of the p.c.i. and the surface. As indicated by the sketch depicted in **Figure 4**, the wettability of the polymer-covered metal surfaces is dominated by rather hydrophobic molecular moieties. In detail, **Figure 4** shows two time-steps of the concomitantly occurring association processes of the p.c.i. molecules in water and at the presence of a hydrophilic surface like, for instance, a hydroxylated magnesium oxide surface. The rounded moieties in the sketches represent the superatoms or beads used for the mesoscale DPD simulation. It is worthwhile mentioning that each one of the DPD beads representing water comprise three water molecules but are not shown for clarity. Moreover, p.c.i. aggregates on the hydrophilic surface may incidentally result to be positioned close to the walls of the simulation cell; then they will be depicted in two seemingly separated parts due to the periodic boundary conditions applied during the simulation. In total, the simulation cell contains ten p.c.i. molecules. The DPD calculations reveal the chronology of the adsorption of amphiphilic polymers: following an association of several molecules in the liquid medium, the associates become adsorbed. That is in contrast to the behaviour for anionic low-molecular surfactants like sodium dodecyl sulfonate (SDS) [30] at metal oxide surfaces, which is effected by the adsorption of single anions followed by a subsequent association and formation of hemimicelles. However, the simulations do not yet reveal the minimum time needed for polymer adsorption in a closed layer or, technologically even more relevant, the time required until an effective protection of the metal surface is secured. In the subsequent sections, an experimental approach to locate such time scale for the p.c.i. adsorption on magnesium will be presented.

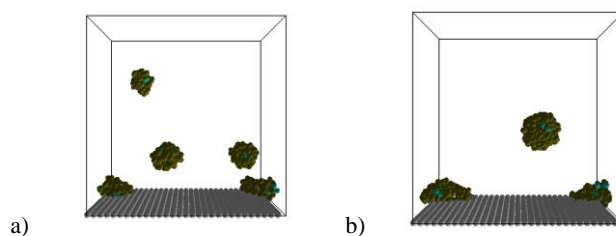


**Figure 4.** Two time-steps during the association of polymeric corrosion inhibitor (p.c.i.) molecules in water and in presence of a hydrophilic surface as revealed by Dissipative Particle Dynamics (DPD) simulations. The water solvent beads are not shown for clarity. In total, the simulation cell contains ten p.c.i. molecules. In the simulation cell depicted on the left side (image a), each aggregate in the aqueous formulation contains two p.c.i. molecules and the aggregate adsorbed on the hydrophilic surface contains four p.c.i. molecules. A later time-step of the simulation (image b) reveals p.c.i. agglomeration in the water phase.

### 3.2. Contact Angle

The static contact angle was measured by establishing the tangent (angle)  $\theta$  of the water drop with a solid surface at the base as shown in [Error! Reference source not found.](#). The AM50 substrate was freshly emiered and it was immersed in the suspension p.c.i. formulation during 3 min, 30 min and 3h; after this treatment the contact angle was measured. The freshly emiered substrate shows high wettability ( $\theta < 25^\circ$ ); contact-angle average values from different immersion times in the p.c.i. formulation are depicted in **Figure 5.a**.

The drops were observed not to be round but more or less elongated, and this finding is attributed to the influence of the roughness of the emiered substrate which is lower along the grooves than perpendicular to the grooves. For the sample obtained after an immersion of 3 min, a clearly higher contact angle than observed for the freshly emiered surface was found. This indicates a change from a highly hydrophilic to a more hydrophobic surface with a lower surface energy as a consequence of the immersion in the p.c.i. formulation.

As references for a substrate wettability, a Silicon wafer and a glassy carbon substrate were used, and contact angle of  $52^\circ$  measured for the silicon wafer indicated that it has got a more hydrophilic surface than the glassy carbon featuring a contact angle of  $71^\circ$ .

Contact angle performed with AM50 samples immersed in the p.c.i. formulation for 3 min up to 3 h did not reveal significant changes of the surface wettability depending on the immersion time.

### 3.3. Aerosol Wetting Test

Like the contact angle (CA) measurements, the Aerosol Wetting Test (AWT) measurements are based the contact between water droplets and substrate surfaces. While the CA measurements are done considering the side view according to different viewing directions on elongated drops, the measurements in the ATW are done performing a top view imaging of the drops and evaluating the area of these drops. The droplet areas are considered to calculate the drop size using a Rosin-Rammler drop-size distribution fit.

The results obtained at the AWT for samples immersed in water and in the corrosion inhibitor liquid formulation are evidenced by the plot shown in **Figure 5.b**. It may be perceived that for samples immersed just in clean water the drop size obtained after ten seconds of immersion is smaller than the drop size obtained after five seconds of immersion, which is smaller than the drop size for the freshly emerged samples.

On the other hand, for samples immersed in the p.c.i. formulation, a distinct difference of the observed drop sizes as compared to the ones obtained for the freshly emerged sample. This holds true already for the AM50 samples which had been immersed for five seconds. Considering the error bar, of the AWT results, there is not a significant difference between the surface wettability obtained after 5 s or after longer immersion times of up to six hours.

Subsequently, the wettability of the p.c.i. covered AM50 samples will be referenced to the wettability of the Silicon wafer and the glassy carbon (GC) sample used as references. The drop size for the freshly emerged samples, in both cases, were almost the same as obtained for the Silicon wafer sample, considered as the hydrophilic reference sample. The drop size obtained for the Glassy Carbon (GC) sample, the hydrophobic reference, was close to the drop size of the AM50 sample immersed for ten seconds in water. . The AM50 samples immersed in the p.c.i. formulation showed clearly lower droplet sizes in the AWT. Neither the average droplet size nor the width of the droplet size distribution were observed to significantly depend on the time of immersion. The categorization of the wettability based on these results is consistent with the one based on the results obtained in the Contact Angle measurements.

Remarkably, the immersion in a p.c.i. formulation changed the mean droplet size after an immersion as short as five seconds. That indicates that the p.c.i. in the aqueous formulation rapidly changes the wettability of the AM50 surface.

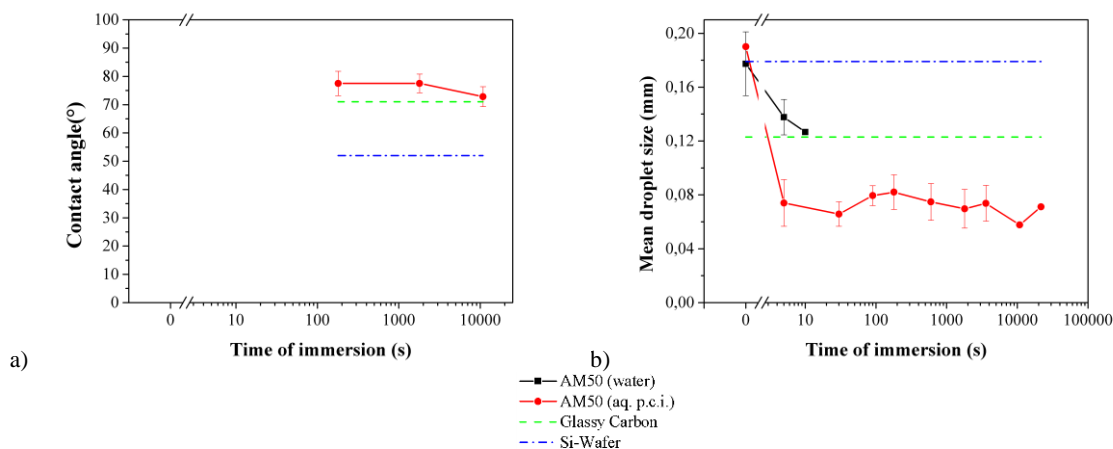


**Figure 5. a)** Contact Angle variation and **b)** mean droplet sizes obtained from Aerosol Wetting Test measurements after different immersion times in clean water or, respectively, in an aqueous p.c.i. formulation.

The observations done may indicate a change of the wettability of AM50 surfaces upon immersion of only five seconds. Such surface modification may be related to a layer formation on the surface of the AM50 samples. On freshly emerged AM50 samples exposed to air, probably an oxide layer is formed, as the magnesium is highly reactive with oxygen, and upon immersion in water a hydroxylated surface layer may be formed as magnesium is highly reactive with water. For samples immersed in aqueous p.c.i. formulation, the change of the



wetting behavior can be explained by the formation of a polymer layer in less than five seconds of immersion. As indicated by the results of the DPD simulation, in contact with the aqueous p.c.i. formulation, an adsorption of the amphiphilic molecules on the surface may occur.

As the AWT results refer to the layer most on the top of the surface, it is possible to affirm that modifications on the surface happened within five seconds of immersion. After this time, there is not any huge difference between the samples immersed in the p.c.i. suspension, even though longer times of immersion might imply more polymer adsorption. Therefore, subsequently investigations referring to the possible corrosion protection properties of such layer will be reported. Moreover, OSEE and XPS analysis were done to evaluate a deeper depth of the surface, to verify the oxide layer formation and the polymer layer deposition, and also to evaluate changes in the polymer layer that could have happened with longer immersion times.

### 3.4. Hydrogen bubble formation test (H<sub>2</sub>BT)

The hydrogen bubble formation due to the reaction of water and the magnesium alloy at especially active sites was monitored. After emerying, the AM50 substrate surface imaged with Laser Scanning Confocal Microscopy (LSCM) as shown in **Figure 6.a** reveals grooves resulting from the emerying treatment. Moreover, elevated and some micrometer wide particulate structures are evidenced. They are interpreted to be harder and, thus, more wear-resistant than the surrounding matrix. They are attributed to intermetallic phases like, for instance, the  $\beta$ -phase ( $Mg_{17}Al_{12}$ ), of AM50. Such intermetallic phases may be more noble than the surrounding matrix material and form local galvanic cells at which the corrosion is promoted locally. The results obtained in the Hydrogen Bubble Formation Test (H<sub>2</sub>BT) are shown in **Figure 6.b**. It is possible to observe that on an unprotected AM50 surface immersed in water hydrogen bubbles appear after approximately three seconds, and the area density of bubbles generated on the surface of the AM50 is around 100 per mm<sup>2</sup>. Such hydrogen bubble area density fairly accords with the interpretation of the LSCM image displayed in **Figure 6.a** which was tentatively explained to show one area of intermetallic phases within 0.01 mm<sup>2</sup>. When the aqueous p.c.i. formulation is applied over the sample instead of clean water, the hydrogen bubble formation decreases significantly. This holds true as well for the onset of bubble formation which is delayed to 120 seconds as for the area density of hydrogen bubbles which is approximately two orders of magnitude lower when compared to the immersion in clean water. These observed differences mean that the adsorbing p.c.i. postpones the time after which the first bubbles appear by a factor of 40.

Assuming that the incidence of the hydrogen bubbles is related to the galvanic corrosion at noble intermetallic phases exposed at the surface of magnesium alloys, in clean water an electrochemical contact between the two metal phases and the aqueous electrolyte occurs. The observation based on the AWT indicates that with the application of the p.c.i. on the surface of the AM50 a polymer layer is formed within less than five seconds. On the other hand, the results obtained in the H<sub>2</sub>BT suggest that this layer effectively acts against galvanic corrosion after latest three seconds. The respective layer covers the surface of the alloy in a way that the contact between the metal phases and the electrolyte is diminished. Concluding, the adsorption of the polymer avoids the hydrogen formation and consequently induces corrosion protection.

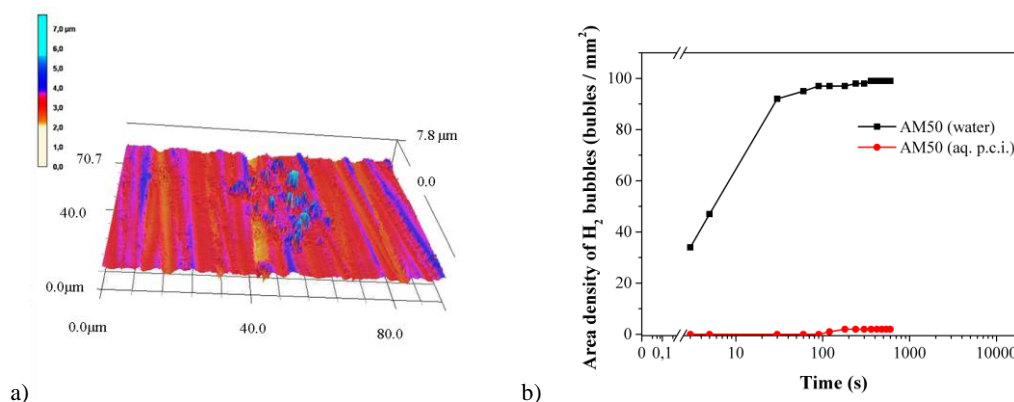


**Figure 6.a)** Confocal microscopy (LSCM) image of a freshly emerged AM50 and **b)** incidence of hydrogen bubbles on AM50 samples in clean water and, respectively, an aqueous p.c.i. formulation as a function of immersion time.

### 3.5. Optically Stimulated Electron Emission (OSEE)

Effects of layer formation of layers and films on the surface of AM50 samples as a consequence of the immersion in water or in aqueous polymeric corrosion inhibitor (p.c.i.) formulations were investigated using Optically Stimulated Electron Emission (OSEE). The plot displayed in **Figure 7.b** represents the results obtained with the OSEE technique.

The immersion in water causes a very steep and fast loss of OSEE signal within some seconds of immersion. After five seconds of immersion, the OSEE intensity decays by a half, and after 20 seconds of immersion no emission is found. This is interpreted as an indication of the formation of a hydroxide reaction layer on AM50. On the other hand, when samples are treated with the aqueous p.c.i. formulation, significant OSEE signals are detected until reaching an immersion time of three hours. After six hours of immersion in the polymer formulation, no emission is found. Observing the course of OSEE signal with an increasing time of immersion, it is also noticeable that the upon prolonged immersion in the p.c.i. formulation the OSEE signal decreases. This is interpreted to be due to layers on the AM50 surface which grow in thickness with time. If a less photo-emitting layer system is formed, its effect on the OSEE signal will be the higher the thicker the layer system is and the more electrons emitted from the metallic sample are scattered.

These OSEE results show, for all situations, a decrease of intensity when immersed samples are compared to the freshly emerged surface of the alloy. Both upon immersion in clean water and upon immersion in the aqueous p.c.i. formulation, a layer is formed on the metal surface. Considering the differences of wettability identified using the AWT, different layers are formed in contact with clean water and, respectively, in contact with the p.c.i. formulation. By means of OSEE, a slower layer growth is indicated for the immersion in the p.c.i. formulation as compared to the immersion in clean water. However, a differentiation cannot be performed concerning the chemical composition of formed layer system, since both thinkable layers, namely hydroxide and polymer layers, are less photo-emitting than the metallic surface of the alloy, a finding also reported in the studies of aluminum surfaces by Romand et al. [9].

From the OSEE investigations kind of an efficiency concerning the corrosion protection properties of the adsorbing p.c.i. can be obtained. Based on time until the OSEE signal of an AM50 surface having been immersed vanishes, the alloy protection is around 1000 times more effective in the presence of the p.c.i. as compared to clean water. The technique can also follow, with quick and simple procedures, the formation and growth of layers on the alloy surface. For a clear characterization of this layer system, a spectroscopic surface analytical technique will be used.

### 3.6. X-ray Photoelectron Spectroscopy (XPS)

Finally, X-ray Photoelectron Spectroscopy (XPS) investigations of AM50 surfaces obtained after immersion were performed with the samples selected based on the inexpensive and fast characterizations achieved with

online-capable techniques. The most relevant results obtained using are depicted in the **Figure 7.a**. A set of two plots refer to the concentration ratio between metallic magnesium species and the total of magnesium species found for samples immersed in water and, respectively, in the aqueous p.c.i. formulation. Moreover, the concentration ratio between carbon and magnesium species for the samples immersed in the p.c.i. formulation is displayed.

For the immersion in water, a clear decrease by more than 70 % of the metallic magnesium content is observed upon less than one minute of immersion. This decrease is due to the formation of a hydroxide layer resulting from the formation of undissolved magnesium species in contact with water.

However, when samples are immersed in the aqueous formulation of p.c.i., two concurrent effects may happen: the oxidation of the alloy and the chemisorption of the polymeric layer. Therefore, the respective signals are discussed. First, decrease of the ratio between metallic magnesium species and the total of magnesium species is less than 50 % even after six hours of immersion. That indicates that the increase of the hydroxide layer thickness on magnesium is drastically diminished in the presence of the p.c.i. as compared to the immersion in pure water. The oxide layer formed is thin, in the range of a few nanometers. Second, the content of carbon species increases with time, and it is most pronounced after times of immersion longer than 30 minutes. Even after only 30 seconds of immersion in the p.c.i. formulation, a thin organic film can be detected. As for longer times the relative content of carbon species increases while the relative content of magnesium within the topmost surface region decreases, it is noticeable that a layer of carbon-containing species is growing on top of the AM50 surface.

The time-dependent behavior dominated by the increase of organic species on the AM50 surface is somewhat inversely proportional to the behavior of OSEE signal which decays. Within shorter times of immersion, the OSEE intensity decay is less steep, as the growth of carbon content. For times higher than three hours, however, the OSEE signal falls quickly as the polymeric layer becomes thicker and more close-packed.

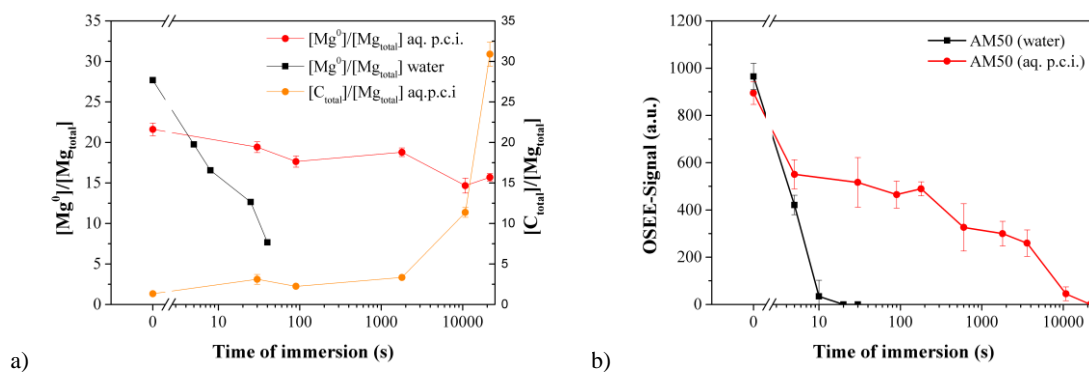


**Figure 7.** Effects of immersing AM50 in clean water and, respectively, a formulation of polymeric corrosion inhibitor (p.c.i.): **a)** Ratios of  $[Mg^0]/[Mg_{total}]$  and  $[C_{total}]/[Mg_{total}]$  as function of immersion time, obtained by XPS; **b)** OSEE signal as a function of immersion time

## 4. Conclusions and Outlook

A combination of several techniques for instantly monitoring or elaborately analyzing the surface state of magnesium was applied in order to characterize the performance of new polymeric corrosion inhibitors. Fast online-capable and large-scale techniques like Aerosol Wetting Test and Optically Stimulated Electron Emission and, additionally, an inexpensive microscopic hydrogen bubble test for following effects of galvanic corrosion processes occurring at active sites were employed to investigate characteristic properties of polymeric corrosion inhibitors on a time-scale between some seconds and a few hours. Targeted samples selected based on the thus obtained results were characterized using an established technique like X-ray Photoelectron Spectroscopy.

The surface-sensitive techniques allow to indicate early occurring degradation and, respectively, corrosion inhibition effects. Following the combined investigations, the new polymeric corrosion inhibitors become ad-

sorbed on the freshly emiered AM50 surfaces within less than three seconds, in a few nanometers thin layer inhibiting galvanic corrosion processes of the AM50 in contact with water. Moreover, a long-term corrosion inhibition effect for at least several hours is obtained in presence of the aqueous formulation of a polymeric corrosion inhibitor. This effect is related to a growing organic layer which becomes closely packed and reaches a thickness of around ten nanometers within some hours.

Ongoing investigations focus on the corrosion protection properties of distinctly thick films with the polymeric corrosion inhibitor when applying accelerated ageing tests like salt spray tests.

## Acknowledgements

The authors thank to Science without Borders (Ciência sem Fronteiras, proc. 88888.021780/2013-00, 88888.021800/2013-00, 88888.020610/2013-00), Coordination of Improvement of Higher Education Personnel (CAPES – Brazil) and Consejo Nacional para Investigaciones Científicas y Tecnológicas de Costa Rica. (CONICIT) for the funding; the German Federal Ministry of Economics and Technology (BMWi) under the ZIM programme (Zentrales Innovationsprogramm Mittelstand- ZIM) and the ‘KABA’ project (funding reference KF2139502 HA9) carried out with Straetmans HighTAC GmbH); Enio B. Adolfo for the sketching on the figure 3; Alexander I. Petzhold for the text review; Dr. Hauke Brüning for the LSCM; and Prof. Dr. Horst-Erich Rikeit and Prof. Dr. Bernd Mayer for steady support and interesting discussions.

## References

- [1] Song, G. (2005) Recent progress in corrosion and protection of magnesium alloys. *Advanced engineering materials*, **7**, 563 – 586. doi:[10.1002/adem.200500013](https://doi.org/10.1002/adem.200500013).
- [2] Song, G. and Atrens, A. (2003) Understanding magnesium corrosion: A framework for improved alloy performance. *Advanced engineering materials*, **5**, 837 – 858. doi:[10.1002/adem.200310405](https://doi.org/10.1002/adem.200310405).
- [3] Raja, P.B. and Sethuraman, M.G. (2008) Natural products as corrosion inhibitor for metals in corrosive media: A review. *materials letters*, **62**, 113 – 116. doi:[10.1016/j.matlet.2007.04.079](https://doi.org/10.1016/j.matlet.2007.04.079).
- [4] Hu, R.-G., Zhang, S., Bu, J.-F., Lin, C.-J. and Song, G.-L. (2012) Recent progress in corrosion protection of magnesium alloys by organic coatings. *Progress in Organic Coatings*, **73**, 129 – 141. doi:[10.1016/j.porgcoat.2011.10.011](https://doi.org/10.1016/j.porgcoat.2011.10.011).
- [5] Ishizaki, T., Masuda, Y. and Sakamoto, M. (2011) Corrosion Resistance and Durability of Superhydrophobic Surface Formed on Magnesium Alloy Coated with Nanostructured Cerium Oxide Film and Fluoroalkylsilane Molecules in Corrosive NaCl Aqueous Solution. *Langmuir*, **27**, 4780 – 4788. doi:[10.1021/la2002783](https://doi.org/10.1021/la2002783).
- [6] Liu, Y., Yu, Z., Zhou, S. and Wu, L. (2006) Self-assembled monolayers on magnesium alloy surfaces from carboxylate ions. *Applied Surface Science*, **252**, 3818 – 3827. doi:[10.1016/j.apsusc.2005.05.072](https://doi.org/10.1016/j.apsusc.2005.05.072).
- [7] Smith, T. (1983) Surface Quality Unit for Inspection by Nondestructive Testing (SQUINT). In: *National SAMPE Technical Conference, Fall*.
- [8] Lee, T.-H. (1990) Selection of lubricants for metal evaporated tape. *Magnetics, IEEE Transactions on*, **26**, 171 – 173. doi:[10.1109/20.50525](https://doi.org/10.1109/20.50525).
- [9] Romand, M., Gaillard, F., Charbonnier, M., Prakash, N.S., Deshayes, L. and Linossier, I. (1995) Adhesion Science and Surface Analysis. Typical Examples. *The Journal of Adhesion*, **55**, 1 – 16. doi:[10.1080/00218469509342403](https://doi.org/10.1080/00218469509342403).
- [10] Zatsepin, A.F., Fitting, H.-J., Kortov, V.S., Pustovarov, V.A., Schmidt, B. and Buntov, E.A. (2009) Photosensitive defects in silica layers implanted with germanium ions. *Journal of Non-Crystalline Solids*, **355**, 61 – 67. doi:[10.1016/j.jnoncrysol.2008.08.025](https://doi.org/10.1016/j.jnoncrysol.2008.08.025).
- [11] Parker, B.M. and Waghorne, R.M. (1991) Testing epoxy composite surfaces for bondability. *Surface and Interface Analysis*, **17**, 471 – 476. doi:[10.1002/sia.740170710](https://doi.org/10.1002/sia.740170710).
- [12] Rider, A.N. (2006) Prebond Inspection Techniques to Improve the Quality of Adhesive Bonding Surface Treatments.
- [13] Schlanger, S. and Epstein, G. (1991) Optically stimulated electron emission (OSEE): A non-invasive technique for contamination detection. *Review of progress in quantitative nondestructive evaluation*, 589 – 595.
- [14] Hindin, B. and Ventresca, C. (1994) Metal-Detergent/Cleaner Compatibility.
- [15] J.R. Davis (2000) Understanding the Corrosion Behavior of Aluminum. Chapter 2. In: Davis, J. R., Ed., *Corrosion of aluminum and aluminum alloys*, ASM International, Materials Park, U.S.A., 26–44.
- [16] Kohli, R. and Mittal, K.L. (2013) Developments in surface contamination and cleaning: fundamentals and applied aspects, Elsevier.

- [17] Kwok, D.Y. and Neumann, A.W. (1999) Contact angle measurement and contact angle interpretation. *Advances in colloid and interface science*, **81**, 167 – 249. doi:10.1016/S0001-8686(98)00087-6.
- [18] Islam, M.S., Tong, L. and Falzon, P.J. (2014) Influence of metal surface preparation on its surface profile, contact angle, surface energy and adhesion with glass fibre prepreg. *International Journal of Adhesion and Adhesives*, **51**, 32 – 41. doi:10.1016/j.ijadhadh.2014.02.006.
- [19] Ruiz-Cabello, F.J., Rodríguez, M.A. and Cabrerizo-Vílchez, M.A. (2014) Equilibrium contact angle or the most-stable contact angle? *Advances in colloid and interface science*, **206**, 320 – 327. doi:10.1016/j.cis.2013.09.003.
- [20] Zografi, G. and Johnson, B.A. (1984) Effects of surface roughness on advancing and receding contact angles. *International journal of pharmaceutics*, **22**, 159 – 176. doi:10.1016/0378-5173(84)90019-X.
- [21] Goddard, J.M. and Hotchkiss, J.H. (2007) Polymer surface modification for the attachment of bioactive compounds. *Progress in polymer science*, **32**, 698 – 725. doi:10.1016/j.progpolymsci.2007.04.002.
- [22] Rahimi, M., Fojan, P., Gurevich, L. and Afshari, A. (2014) Effects of aluminium surface morphology and chemical modification on wettability. *Applied Surface Science*, **296**, 124 – 132. doi:10.1016/j.apsusc.2014.01.059.
- [23] Wilken, R., Markus, S., Amkreutz, M., Tornow, C., Seiler, A., Dieckhoff, S. and Meyer, U. (2008) Method and device for testing a surface quality. EP1893974 B1.
- [24] (ENCOMB) Extended Non-Destructive Testing of Composite Bonds (2012) 1st Periodic Report(grant agreement no 266226), Saarbrücken, Germany, 43 – 46.
- [25] Hoffmann, M., Stübing, D., Brune, K., Dieckhoff, S. and Markus, S. (2013) Quality assurance concepts for adhesive bonding of aircraft composite structures by extended NDT. *3rd International Conference of Engineering Against Failure (ICEAF III)*, Kos, Greece, 26-28 June 2013.
- [26] Tornow, C., Brune, K., Schlag, M., Hoffmann, M., Stübing, D. and Dieckhoff, S. (2014) Quality assurance concepts for adhesive bonding of composite aircraft structures: Characterisation of adherend surfaces by extended NDT. *10th European Adhesion Conference (EURADH 2014)*, Alicante, Spain, 22-25 April 2014.
- [27] Straetmans High TAC GmbH Additive G50. <http://hightac.de/g50/InfoAdditiveG50.pdf>
- [28] Cavalcanti, W.L., Brinkmann, A., Noeske, M., Buchbach, S., Straetmans, F. and Soltau, M. (2012) Dual-purpose defenders: Organic polymers protect metals in both thin layers and coatings. Anticorrosive systems. *European Coatings Journal*, **10**, 1 – 4.
- [29] Brune, K., Lima, L., Noeske, M., Thiel, K., Tornow, C., Dieckhoff, S., Hoffmann, M. and Stübing, D. (2013) Pre-bond Quality Assurance of CFRP Surfaces Using Optically Stimulated Electron Emission. *3rd International Conference of Engineering Against Failure (ICEAF III)*, Kos, Greece, 26-28 June 2013.
- [30] Somasundaran, P. and Fuerstenau, D.W. (1966) Mechanisms of alkyl sulfonate adsorption at the alumina-water interface. *The Journal of Physical Chemistry*, **70**, 90 – 96.